

Ultra-short pulses propagation through a strongly scattering medium

Cécile Calba¹, Thierry Girasole², Claude Rozé³, Loïc Méès⁴

1: UMR 6614-CORIA, CNRS, Université et INSA de Rouen, FRANCE, calba@coria.fr

2: UMR 6614-CORIA, CNRS, Université et INSA de Rouen, FRANCE, girasole@coria.fr

3: UMR 6614-CORIA, CNRS, Université et INSA de Rouen, FRANCE, roze@coria.fr

4: UMR 6614-CORIA, CNRS, Université et INSA de Rouen, FRANCE, mees@coria.fr

Abstract Forward light scattering of femtosecond pulses through strongly scattering media is investigated experimentally and numerically. The temporal separation between ballistic light and scattered light is exhibited and used to perform optical depth measurements up to 22, corresponding to transmission factor of about 10^{-9} . Quantitative comparisons between experiments and Monte Carlo simulations show a good agreement. Computations are based on a semi Monte Carlo method including polarization effects. Temporal forward scattered light evolutions with concentration and particle size are presented.

1. Introduction

Optical techniques are widely applied to two phase flow characterization, in research area as well as in industry. They generally offer a precise and non intrusive way to measure particle sizes, concentration, or velocity fields. However, common optical techniques are limited in term of particle concentration. Diffraction based particle sizer are limited to transmission factor larger than 50 % and alternative techniques, such as PDA, hardly work with transmission factor lower than 10 %. This limitation is due to multiple scattering effects. Indeed, information contained in scattered light is generally inversed assuming only single scattering processes and is progressively scrambled and destroyed when the particle concentration and the multiple scattering processes increase. Even if multiple scattering effects can sometimes be taken into account by introducing correcting factors, this limitation still exists and is just weakly shifted.

In forward scattering configuration, a way to overpass this limitation consists in marking the incident photons, in order to separate the ballistic light which contains information, from scattered light. Most advanced method are based on a polarization modulation, allowing to extract ballistic light from multiple scattering. However these techniques are limited to stationary media, and can not be applied to media in rapid evolution as often encountered in fluid mechanics.

An alternative and promising way to investigate strongly scattering media consists in using ultra-short light pulses and an associated time resolved detection. During 100 fs, which is nowadays a current pulses duration for mode-locked lasers, light travel is only 30 μm in air and 20 μm in water. Resolution at this time scale may then offer a way to distinguish photons with optical paths differences of a few ten microns. In a strongly scattering medium, multiple scattered photons are time delayed, due to the extra-paths they experience between the scattering particles they encounter. A femtosecond time scale detection may then isolate the ballistic photon, directly transmitted through the medium (without any interaction), from scattered light. Moreover, the temporal evolution of transmitted light, which is related to photon travel paths in the medium, may contain an information on the medium itself.

The potential of ultra-short pulses to investigate strongly scattering media have been considered in previous works, essentially motivated by bio-medical potential applications. Backscattering of femtosecond pulses has been studied in Hauger *et al*, where experimental results are compared with Monte Carlo simulation. The forward scattering case is considered in Guo *et al* at a larger time scale (60 ps pulses). But to measure both ballistic light and scattered light and exhibit their temporal

separation, a shorter time resolution is needed. A qualitative comparison between experiments and computation can be found in Podgaetsky *et al*, where femtosecond pulses and a streak camera with 1.5 ps time resolution are associated to measure the forward scattering by a strongly scattering medium.

In this paper, time resolved light scattering in forward direction by strongly scattering media is studied at femtosecond time scale. Our approach is both experimental and numerical. Simulations based on a semi Monte Carlo method are compared with experimental results, obtained by using intense 100 fs pulses, and an optical cross correlation between a reference pulse and a probe pulse.

2. Monte Carlo simulations

Monte Carlo method has been widely used to simulate light propagation in scattering media. It gives a mathematically accurate statistical solution to the Radiative Transfer Equation. Classically, the light sources are described by a collection of energy quanta, called “photons” for convenience. Each photon is launched from the source, and its trajectory is simulated by comparing drawn random numbers and known probabilities describing individual events (absorption, scattering, ...).

The Monte Carlo method can be easily adapted to simulate time resolved scattering of an ultra-short pulses by a particle cloud, when the particle sizes are small enough with respect to the pulse length (duration \times celerity). The arrival time of each detected photon is then simply related to the travel path it experiences between the scattering particles. When the particle size is greater, the time spent during interaction is no more negligible. Moreover, the pulse spreads out into temporally separated pulses at each interaction (Méès et al 2001; Méès et al 2001). In such a case, a specific Monte Carlo method has been developed (Rozé et al 2003; Calba et al 2006). In this paper, however, we only deal with small particles.

The Monte Carlo approach is an easy way to consider extremely complex phenomena, but it is generally limited by time consuming, especially when considering a small detecting angle. When the collection angle decreases, the number of detected photons decreases, and the number of photons to be launched from the light source to obtain an accurate statistical description of the phenomenon increases very fast, leading to strong limitation in term of time consuming.

In order to increase the number of ‘useful’ photons, we used a semi-analytical Monte Carlo approach (Bruscaglioni et al 1993) which is a mixture between a statistical and an analytical method, but mathematically equivalent to the classical Monte Carlo method. This approach keeps the statistical characteristic of Monte Carlo technique. “Photons” trajectories are built from drawing numbers and known physical laws (single scattering processes in our case). In classical Monte Carlo method, the detected signal is built from photons colliding with the detectors. Other photons do not contribute to the detected signal and it entails a lost of computation time. In semi-Monte Carlo method, the contribution to the detected signal is computed at each photon collision. This contribution is evaluated from the relative position of detector and photon, the phase function of the scattering particle, and the probability for the photon to reach the detector without being scattered or absorbed by the medium (distance and extinction coefficient). The saving of time, using the semi Monte Carlo method instead of the classical Monte Carlo method depends on the configuration under study. In the case under study, computation time decreases by a factor 8000.

Using the probability density functions to govern the movement of the photon, the semi-MC method calculates the small but finite fraction that will be firstly scattered through an angle $(\vec{\Omega}_n, \vec{\Omega}_s)$ toward a direction $\vec{\Omega}_s$, which lies within the small solid angle $\Delta\Omega_s$ subtended by the detector area at point \vec{x}_n , then proceed from point \vec{x}_n to the detector without any interaction on the medium. The flux collected by the remote detector upon a scattering event at point \vec{x}_n can be written as

$$q_\lambda = \frac{\Phi(\vec{\Omega}_n, \vec{\Omega}_s)}{4\pi} \exp(-k_{ext} x_n) \Delta\Omega_s \quad (1)$$

where $\Phi(\vec{\Omega}_n, \vec{\Omega}_s)$ is the scattering phase function which is assumed constant over the small solid angle $\Delta\Omega_s$ and gives the fraction of the photon from the direction $\vec{\Omega}_n$ scattered into an element of solid angle $\Delta\Omega_s$ about the direction $\vec{\Omega}_s$. The item $\exp(-k_{ext} x_n)$ represents the probability that the scattered photon through $(\vec{\Omega}_n, \vec{\Omega}_s)$ will then be transmitted from point \vec{x}_n to the border of the medium (a distance x_n) along the direction $\vec{\Omega}_s$ with no further interaction. k_{ext} is the extinction coefficient for the particles.

Finally, in order to simulate properly the following experiments, our program has been extended to take into account polarisation effects. This extension simply consists in transporting two polarization components instead of an energy quantum but leads to extra computations at each interaction and to an increasing of the time consuming by a factor 4 (2 minutes on a standard PC for each curve presented in section 6).

3. Configuration under study

The strongly scattered media under study are constituted by calibrated polystyrene particles immersed in water and placed in a rectangular glass cell, with variable lengths L (1, 2 and 5 mm). The particles complex refractive index is $m=1.58-0.001i$, at 800 nm and the particle size varies around 1 μm . The water refractive index is $n=1.33-ki$ where the imaginary part k will be defined later. The cell walls thickness is 1 mm and refractive index is 1.5. The illuminating pulsed beam diameter is 5 mm, its duration 100 fs, and its carrier wavelength is 800 nm, corresponding to the experimental set-up, to be later introduced. The beam polarization is vertical. Detection is assumed to be angular and limited to the vertical polarization component. Following the experimental set-up, the collection angle is $\Delta\Omega=2\pi.\Delta\theta$, with $\Delta\theta$ about 0.05° (Fig. 1).

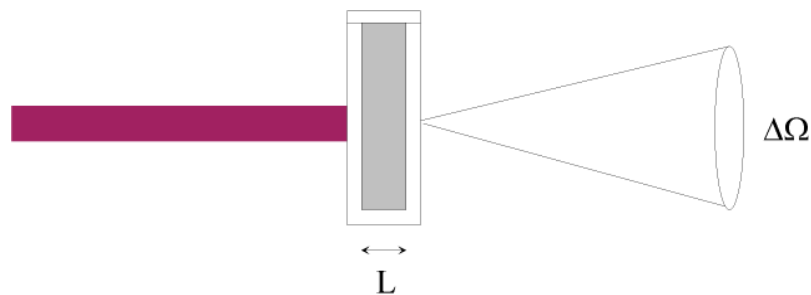


Fig. 1 Configuration under study

4. Experimental set-up

The experimental set-up is presented in Fig. 2. The incident pulsed laser consists of Ti:Sa regenerative amplifier providing 100 fs pulses at 1 KHz repetition rate, at 800 nm carrier wavelength. Energy per pulse is 0.8 mJ. The laser pulse is separated in two parts, named as reference and probe pulses. The probe pulse travels through an adjustable delay line and illuminates the scattering medium which consists of a latex solution of 1 μm particles with variable concentrations. The scattered and reference pulses are then correlated in a BBO crystal, in a non collinear configuration and the temporal signal is recovered by moving the delay line, i.e. by changing the time delay between reference and probe pulses. The two pulses are focused on a BBO

crystal by means of a $f=150$ mm focal length lens. The distance between the BBO crystal and the lens and the distance between the sample and the lens are equal to f , ensuring an angular selection of the light scattered from the sample. Each pulse generates a doubled-frequency signal without direction modification. The superposition of the two pulses generates a frequency doubling in an intermediate direction between the two incident pulses propagation directions. A spatial selection is then used to record only the 400 nm signal issued from the superposition of the two pulses on a Photo-Multiplier. The reference beam is, as the incident beam, vertically polarized. Only the vertical polarization component of the scattered beam contributes to the frequency doubling and is then recorded.

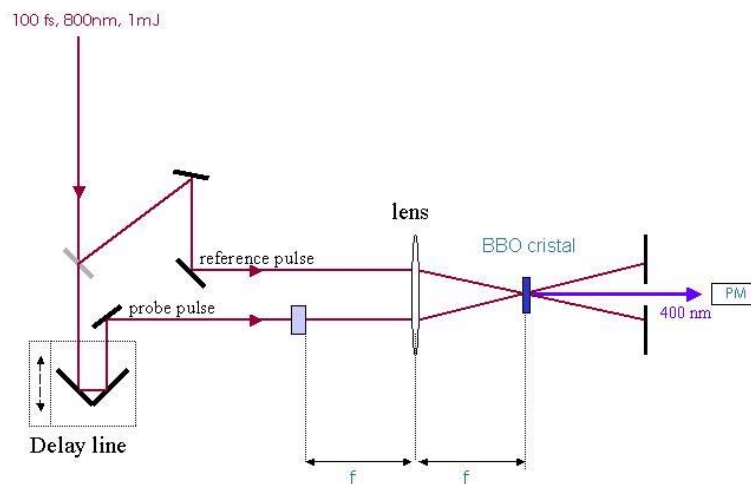


Fig. 2 Experimental set-up

The system is calibrated, using different sets of Neutral Density Filters (ND) and a pure water cell instead of the latex cell. Attenuation of direct light in water and loss due to reflection at the cell walls are then taken into account during the calibration process and are then not considered in simulations results presented later. Some ND are sometimes maintained before the latex cells, reducing the incident and transmitted beam intensities, in order to ensure that the recorded signal remains in the same order of magnitude for lower particle concentrations. The whole set-up is driven by computer.

5. Concentration measurement from ballistic light

Figure 3 displays the transmitted light through a $1 \mu\text{m}$ latex solution versus time for different particle concentrations. The latex solutions have been obtained by successive dilutions of an initial one whose volume concentration is supposed to be approximately 9.52 % (10% mass concentration).

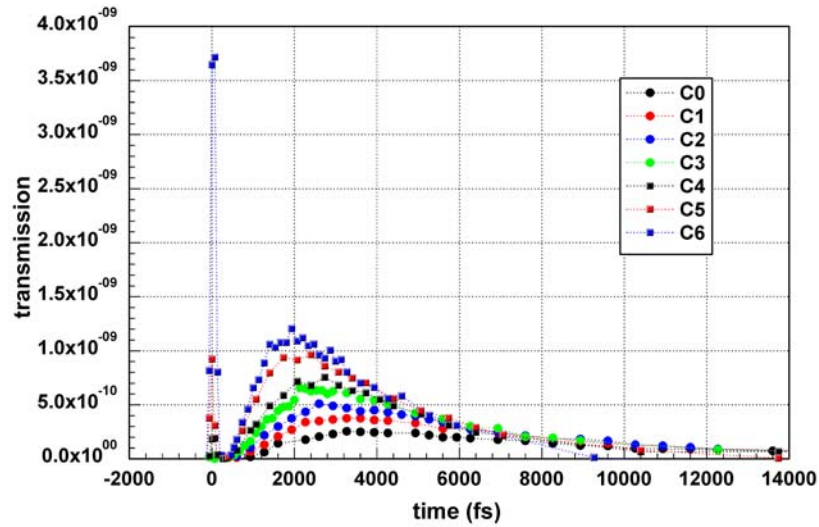


Fig. 3 Transmitted light versus time for decreasing polystyrene particle concentrations from C0 to C6. The cell length is $L=5$ mm for all curves

In figure 3, transmitted signals consist of two intensity peaks. The first one, centered at $t=0$ fs, corresponds to ballistic light (or direct transmitted light). The ballistic peak intensity decreases with the concentration increases (from C6 to C4) and vanishes for greater concentrations (C3 to C0). The second peak corresponds to scattered light, detected with short time delays, corresponding to the extra-paths experienced between the scattering particles. The scattered peak intensity decreases with the concentration increases (from C6 to C0) but slower than the first peak intensity. The time position of the scattered peak maximum depends on the concentration. It moves toward 0 fs (i.e. closer to the ballistic peak) with the concentration decreases. Figure 3, the two peaks are well separated in all cases. The ballistic light is then well isolated from scattered light. The ballistic peak intensity measurement then provides a direct measurement of the optical depth, free from multiple scattering effects. Optical depth is simply deduced by the Beer-Lambert law

$$od = -\ln\left(\frac{I}{I_0}\right) \quad (2)$$

where I is the transmitted intensity and I_0 the incident one.

In case of a mono-sized particles cloud, the particles concentration (m^{-3}) and optical depth are related by

$$od = N \cdot C_{ext} \cdot L \quad (3)$$

where $C_{ext} = C_{ext}(d, m/n, \lambda)$ is the extinction cross section of the particles, function of diameter d , refractive indexes ratio m/n and wavelength λ . For the samples labeled C4 to C6, represented in figure 3, and others (not represented), the ballistic peak intensity has been used to determine a volume concentration. These measured concentrations are compared to the concentrations estimated from the dilution processes in Fig. 4. Corresponding optical depths are in the range 9 to 22. The agreement is good and mainly depends on the quality of the dilution processes.

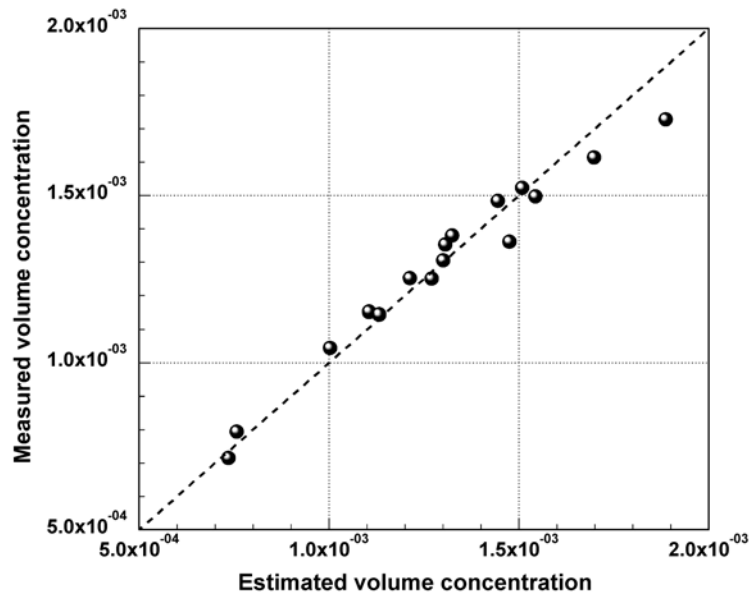


Fig. 4 Concentration measurements from ballistic peak intensities. The measured concentrations are compared with concentrations estimated from dilution processes

6. Comparison between experiments and computation results.

The measured ballistic peak intensity agrees with the Beer-Lambert law. In order to study the contribution of the scattered light, experimental results are now compared to Monte Carlo simulations.

Different parameters are known in our experiments : namely, the particles diameter and the refractive index, the inside length L of the cell. The particles concentration can be determined from ballistic peak intensity when it can be measured (optical depth under 22). The remaining parameters are the collection angle $\Delta\theta$ and the absorption coefficient in water which is non negligible in our experiments. On Figure 5, these two parameters have been adjusted to fit experimental data. The best fit has been obtained for $\Delta\theta=0.065^\circ$, and an absorption water coefficient $K_T=1.5 \times 10^{-4} \text{ fs}^{-1}$, which is equivalent to a coefficient $K_L=665 \text{ m}^{-1}$, or an imaginary part of the water refractive index $k=4.2 \times 10^{-5}$. The absorption coefficient of water can be directly expressed in fs^{-1} because the arrival time of photons is directly related to their travel paths between the scattering particles, in water. We only consider attenuation related to extra paths, because the direct paths (5 mm in water) is already taken into account during calibration. These two parameters adjustments are relatively independent. The maximum of the scattered peak increases with collection angle increasing and with decreasing absorption in water (coefficient K_T). See Figures 6 and 7, which illustrate the influence of these two parameters on simulation results and show that the shape of the scattered peak and in particular its decreasing part slope, only depends on the absorption coefficient. Note that in the following figures (6 to 10), the ballistic peak is truncated to make clearer the scattered peaks evolution. Its maximum value is indicated with an arrow on the figures.

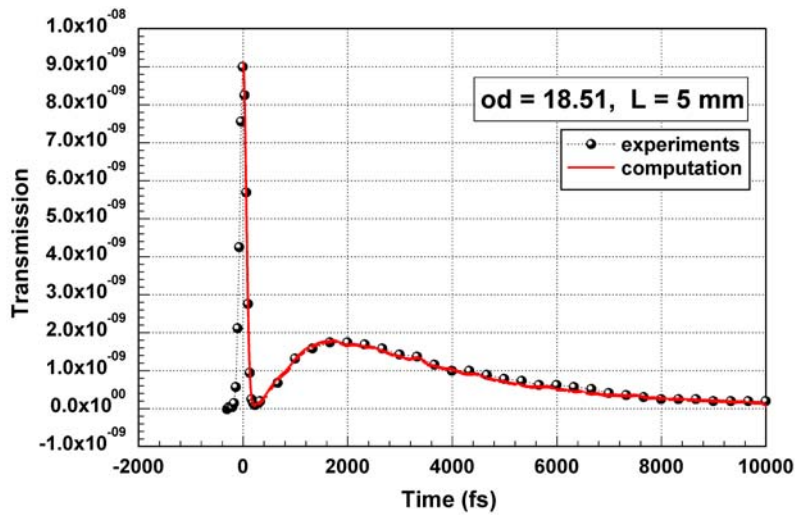


Fig. 5 Comparison between experiments and Monte Carlo simulation for a 5 mm cell. The optical depth $od=18.51$ is measured from the experimental ballistic peak maximum. The particles diameter is $d=1 \mu\text{m}$. The absorption coefficient of water, $K_T=1.5 \cdot 10^{-4} \text{ fs}^{-1}$ and the collection angle $\Delta\theta=0.065^\circ$ correspond to the best fit values

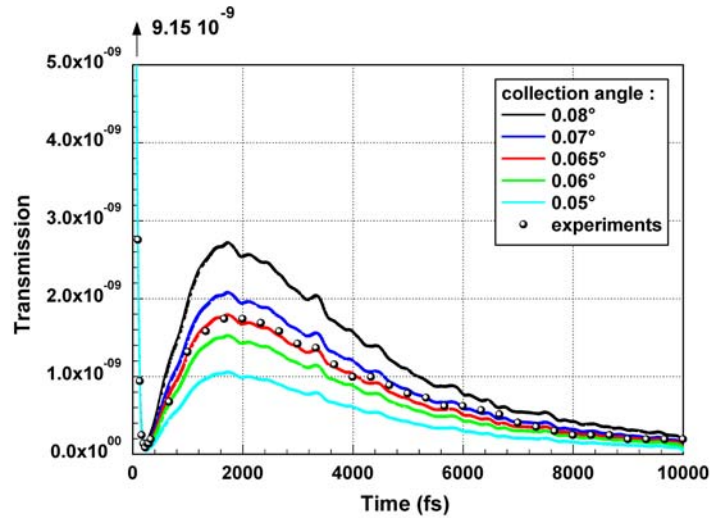


Fig. 6 Influence of collection angles $\Delta\theta$. Other parameters are unchanged with respect to figure 5

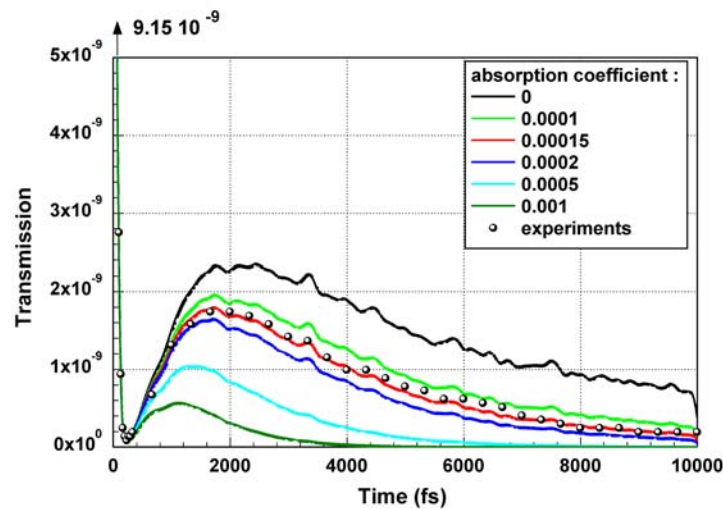


Fig. 7 Influence of the absorption coefficient $K_T (\text{fs}^{-1})$. Other parameters are unchanged with respect to figure 5

Figures 8 to 10 compare experimental results and simulations for different concentrations and cell sizes (1, 2 and 5 mm). The parameters used for simulation are the same than in figure 5. In particular the collection angle and the absorption coefficient remain those determined by best fitting on data displayed in figure 5.

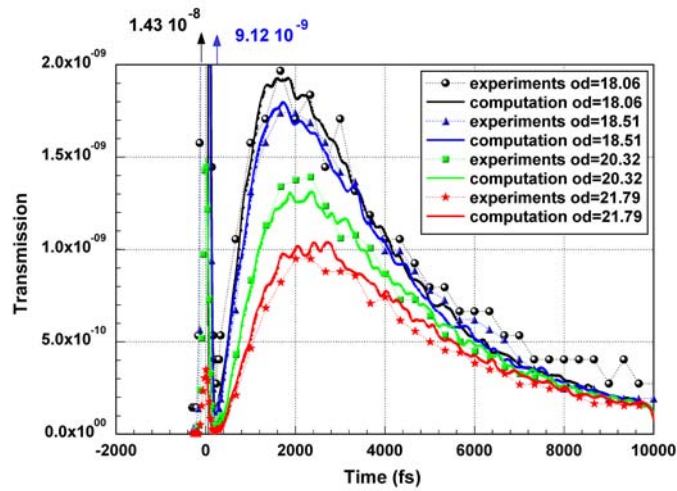


Fig. 8 Comparison between experiments and simulations for 5 mm cell with different particles concentration. Other parameters are unchanged with respect to figure 5

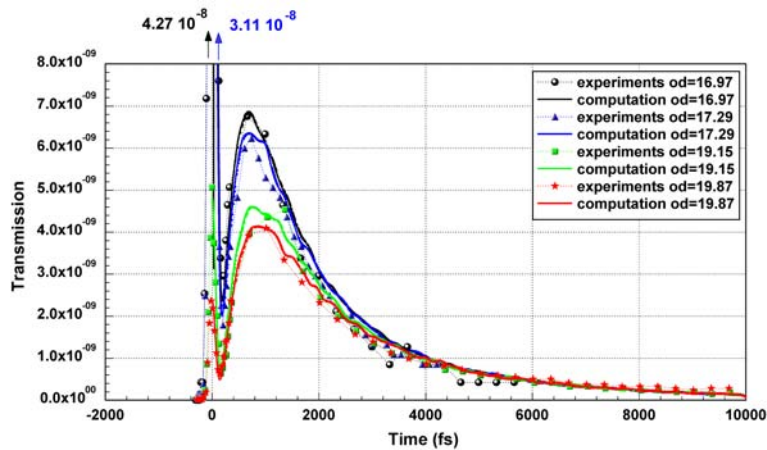


Fig. 9 Comparison between experiments and simulations for a 2 mm cell with various particles concentration. Other parameters are unchanged with respect to figures 5 and 8

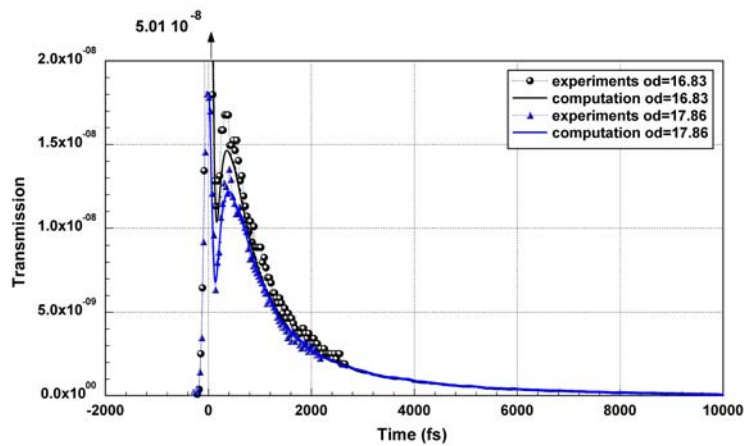


Fig. 10 Comparison between experiments and simulations for a 1 mm cell with various particles concentration. Other parameters are unchanged with respect to figures 5, 8 and 9

Experiments and simulations are still in good agreement in figures 8 to 10, for various concentrations and cell sizes, providing a validation of our Monte Carlo program and numerically determined parameters ($\Delta\theta$ and K_T). In figures 8 to 10, the chosen optical depths correspond to ballistic light and scattered light intensities of the same order, allowing to measure the two peaks together. The corresponding optical depths are smaller for smaller L but corresponding concentrations are greater. The figures also show that the two peaks are closer in time for smaller cell lengths L . The time separation between the two peaks is roughly proportional to the cell length L .

7. Extra computations

In this section, computational results exemplify the influence of the experiment main parameters.

Figure 11 displays the transmitted intensity, in log scale, versus time, for 1 μm latex solution in a 5 mm cell with optical depth as parameter. As previously exemplify by experimental results, the transmitted light in a small collection angle (here $\Delta\theta=0.07^\circ$) is composed by two peaks. The ballistic peak at time 0 fs (our time reference) and a scattered peak, delayed in time. The ballistic peak intensity decreases with increasing optical depth following the Beer-Lambert law. The scattered peak intensity also decreases with increasing optical depth, but slowly than the ballistic peak. As a consequence, the scattered peak intensity is lower than the ballistic peak for optical depths lower than 20, and greater for greater optical depths. As previously noticed, figure 11 shows that the scattered peak time delay increases with increasing optical depth as a consequence of the increasing number of interactions and associated extra-paths.

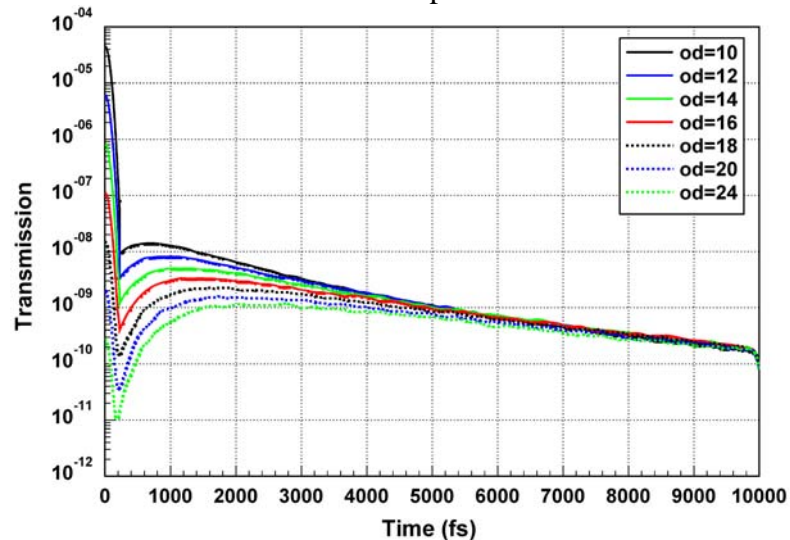


Fig. 11 Transmitted light (in log scale) versus time with optical depth as a parameter. The length of the cell is $L=5\text{mm}$, the particle diameter is $d=1\ \mu\text{m}$, particle refractive index is $n=1.58-0.001i$, absorption coefficient in water is $K_T=1.5\ 10^{-4}\ \text{fs}^{-1}$ and the collection angle is $\Delta\theta=0.07^\circ$

Figures 12a and 12b display the transmitted light intensity versus time, in log scale and linear scale respectively, with the particle diameter as parameter and constant optical depth $\text{od}=20$. The particle diameter varies from 200 nm to 2 μm , other parameters are unchanged with respect to figure 11. Figures 12a and 12b, the ballistic peak intensity is nearly constant, as it should be for a constant optical depth. A small departure from the Beer-Lambert law is however visible for the greater considered particles ($d=1.8\ \mu\text{m}$ and $d=2\ \mu\text{m}$), due to perturbations of the ballistic peak by the scattered peak. The presented results clearly show that the temporal evolution of scattered light

at short time scale contains an information on particle size, at constant optical depth. The second peak intensity increases with increasing particle size and, its maximum location decreases, perturbing the ballistic peak for the greatest particles.

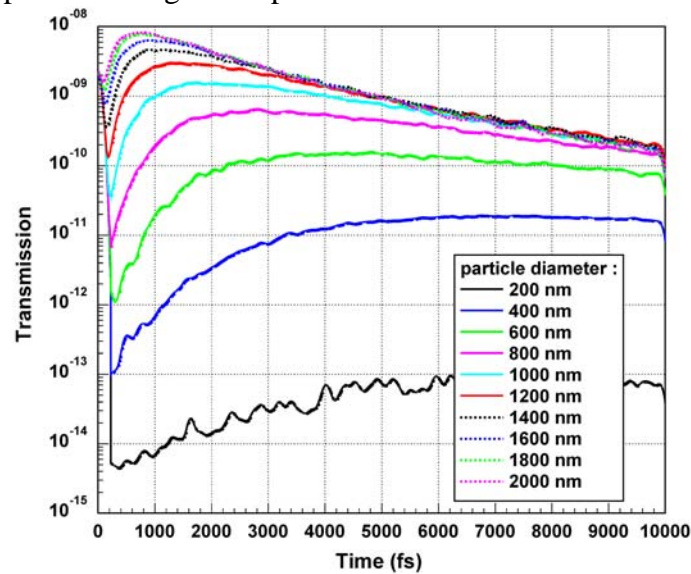


Fig. 12a Transmitted light versus time (in log scale) with the particle size as parameter and a constant optical depth. Other parameters are unchanged with respect to previous figures

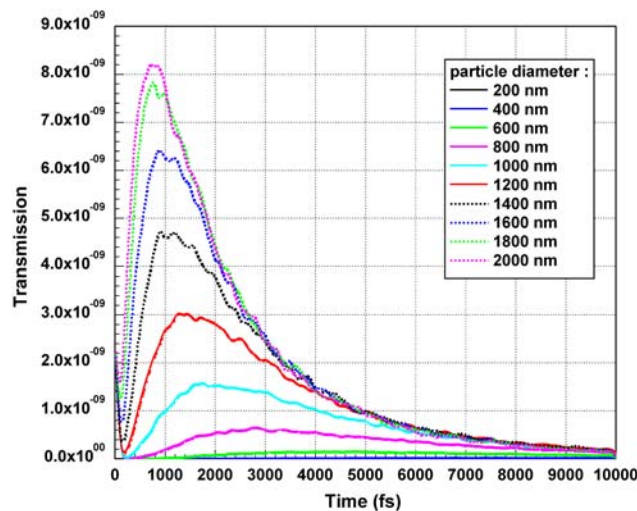


Fig. 12b Transmitted light versus time (in linear scale) with the particle size as parameter and a constant optical depth. Other parameters are unchanged with respect to previous figures

8. Conclusion

We have developed an experimental set-up and an associated simulation program based on a semi Monte Carlo method to investigate the time evolution of scattered light in strongly scattering media impinged by an ultra-short pulse. Presented results demonstrate the potential of such pulses to investigate strongly scattering media. We showed that ballistic light can be isolated from scattered light and provides an optical depth measurement for optical depth up to 22 (about 10^{-9} direct transmission). Moreover, the early scattered light, detected during the first picoseconds after ballistic light has been measured, providing a validation of the Monte Carlo program. Results show that the early scattered light contains an information on particle size, opening ways to particle sizing in strongly scattering media.

References

- Bruscaglioni P, Zaccanti G, Wie Q (1993) Transmission of a pulsed polarized light beam through thick turbid media: numerical results. *Appl Opt* 32:6142-6150
- Calba C, Rozé C, Girasole T, Méès L (2006) Monte Carlo simulation of the interaction between an ultra short pulse and a dense scattering medium: case of large size particles. To be published in *Optics Comm.*
- Guo Z, Aber J, Garetz B A, Kumar S (2002) Monte Carlo simulation and experiments of pulsed radiative transfer. *J. Quant. Spect. Rad. Trans.* 73:159-168
- Hauger C, Baigar E, Wilhelm T, Zinth W (1996) Time-resolved backscattering of femtosecond pulses from scatterin media- an experimental and numerical investigation. *Optics Comm.*, 131:351-358
- Méès L, Gouesbet G, Gréhan G (2001) Scattering of laser pulses plane wave or focused Gaussian beam by spheres. *Appl. Optics* 40:2546-2550
- Méès L, Gouesbet G, Gréhan G (2001) Time-resolved scattering diagrams for a sphere illuminated by plane wave and focused short pulses. *Optics Comm.*194:59-65
- Podgaetsky P M, Tereshchenko S A, Smirnov A V, Vorob'ev N S (2000) Bimodal temporal distribution of photons in ultrashort laser pulse passed through a turbid medium. *Optics Comm.*, 180:217-223
- Rozé C, Girasole T, Méès L, Gréhan G, Hespel L, Delfour A (2003) Interaction between ultra-short pulses and a dense scattering medium by Monte-Carlo simulation : consideration of particle size effect. *Optics Comm.*, 220:237-245